ated Total Reflectance) Fourier Transform Infrared spectra were obtained using a Perkin Elmer Spectrum One spectrometer. Spectra were acquired in the wavenumber range of 500–4000 cm^{-1} at room temperature using KBr with a resolution of 4 cm^{-1}.

4.2. DLS and NMR Analysis

The dynamic light scattering experiments were performed with a Zetasizer NanoZS90 instrument (Malvern Instruments Ltd, Worcestershine, UK). HGAm and GAm were solubilised in distilled water with a concentration of 0.5 mg/mL. Three independent measurements were carried out and used in the analysis of the data.

^{1}H NMR spectra were recorded after solubilization of the sample (11.0 mg) in D_2O (1.0 mL) and the spectra were recorded on a Bruker 400 MHz spectrometer. ^{31}P NMR experiments were recorded as reported in [28]. Briefly, the sample (20 mg) was solubilized in dimethylformamide/pyridine/$CDCl_3$ mixture (0.8 mL; 1.0:1.5:2.5 ratio) and treated with 2-chloro-4,4,5,5-tetramethyl-1,3,2-dioxaphospholane (TMDP) (50 µL) in the presence of n-hydroxy-5-norbornene-2-3-dicarboximide (NHND) (0.9 mmol) as internal standard and chromium(III) acetylacetonate (3.0 mg) as relaxing agent. The spectra were recorded with a Bruker 400 MHz spectrometer overnight.

4.3. Multifrequency Continuous Wave (CW) and Pulse EPR Analysis

EPR spectra were measured with a Bruker ELEXSYS E580E Super Q-FT spectrometer, for CW (X- and Q-band) and pulse Q-band EPR measurements. CW X-band spectra were performed using a Bruker ER 049X microwave bridge with 4122SHQE/0208 cavity. All samples were investigated in powder form. The pyomelanin dry powders were inserted within cylindrical suprasil capillaries (WG-222T-RB, Cortecnet Europe, Les Ulis, France) with ID x OD equal to 1.1 × 1.6 mm and used for both X- and Q-band measurements. The X-band experimental conditions for EPR spectra acquisition were as follows: 9.8 GHz microwave frequency, 0.1 mT modulation amplitude and variable microwave power values in the range (0.0002–210.8 mW) for the power saturation measurements. For an accurate determination of g-factor, two standard markers were used (one with a g = 2.0028 and the other with g = 1.9800). The EDFS spectra of the melanin samples were acquired with a $\pi/2$-τ-π echo sequence. A PFSR sequence was employed for all the measurement of longitudinal relaxation times.

4.4. EC_{50} Determination

The antioxidant activity was determined with the EC_{50} assay carried out with EPR and UV–vis spectroscopies. For the EPR experiments, a stock solution of DPPH 0.4 mM in ethanol with a fixed volume of 100 µL for each sample was used. The antioxidant was dissolved in phosphate buffer with a concentration of 0.127 mg/mL for gallic acid, 1.77 mg/mL for GAm, 0.26 mg/mL for HGAm and 0.59 mg/mL for the gallic acid polymer. For each of these substances an increasing volume of solution ranging from 5 µL to 100 µL was added to DPPH solution to reach a final volume of 200 µL. The DPPH radical signal was monitored for all samples and the DPPH radical in the absence of antioxidant is the reference signal for the scavenger radical percentage determination. After the spectra acquisition, the double integral of each spectrum has been calculated and the scavenger effect percentage was determined using the following formula

$$\text{Scavenger effect } \% \ = \ \frac{A_0 - A_a}{A_0} \cdot 100$$

where A_0 represents the double integral of the DPPH radical without the addition of the antioxidant, A_a is the double integral of the DPPH radical after the addition of antioxidant. Spectra acquisition was run at a fixed time of 15 min after the addition of the antioxidant solution to the DPPH sample.

The antioxidant activity, for the UV–vis DPPH test, was evaluated monitoring the reduction of the DPPH radical peak at 520 nm, for a fixed reaction time of 15 min at T = 298 K

in presence of different concentrations of antioxidants. The samples were prepared with 200 µL of DPPH (0.2 mM–79 µg/mL) and 200 µL of antioxidant at variable concentration. The pyomelanin mimics powder were dissolved in phosphate buffer with a concentration of 0.1 mg/mL for HGAm and 0.16 mg/mL for GAm and gallic acid polymer. For each of these antioxidants an increasing volume of solution ranging from 20 µL to 200 µL was added to the DPPH solution to reach a final volume of 400 µL.

Plotting the DPPH scavenger percentage in function of the log of antioxidant concentration expressed in µg/mL, the EC_{50} value was automatically calculated using GraphPad Prism 5.01. Log (inhibitor) vs. normalized response (variable slope) was the statistical model used for data elaboration of DPPH· assay [39]. The obtained results, for the EPR analysis, are reported in supporting information (Figures S6–S8). All measurements were repeated in triplicate and the standard deviation error for each sample was calculated.

4.5. Scanning Electron Microscopy (SEM) Analysis

The morphological analysis was performed using the Scanning Electron Microscope (SEM; Phenom G2 pure desktop apparatus) (Thermo Fisher Scientific, Waltham, MA, USA) working in the magnification range 20–17,000×.

Supplementary Materials: The following are available online at https://www.mdpi.com/1422-0067/22/4/1739/s1.

Author Contributions: Investigations, formal analysis, data curation, M.A.K., J.C., M.C.B., and D.S.; NMR investigation, formal analysis and data curation E.C. and R.S.; Conceptualization, methodology, formal analysis, writing—original draft preparation, R.P. All authors have participated in writing—review and editing and have read and agreed to the published version of the manuscript.

Funding: CSGI (Consorzio per lo Sviluppo dei Sistemi a Grande Interfase), Florence, Italy and MIUR for the Dipartimento di Eccellenza 2018−2022 grant are gratefully acknowledged.

Institutional Review Board Statement: Not applicable.

Informed Consent Statement: Not applicable.

Data Availability Statement: Data is contained within the article and supplementary material.

Acknowledgments: The authors thank A. Atrei for helpful discussion and DLS measurements.

Conflicts of Interest: The authors declare no conflict of interest.

References

1. Solano, F. Melanins: Skin pigments and much more—types, structural models, biological functions, and formation routes. *New J. Sci.* **2014**, *2014*, 1–28. [CrossRef]
2. D'Ischia, M.; Wakamatsu, K.; Napolitano, A.; Briganti, S.; Garcia-Borron, J.C.; Kovacs, D.; Meredith, P.; Pezzella, A.; Picardo, M.; Sarna, T.; et al. Melanins and melanogenesis: Methods, standards, protocols. *Pigment Cell Melanoma Res.* **2013**, *26*, 616–633. [CrossRef] [PubMed]
3. Turick, C.E.; Knox, A.S.; Becnel, J.M.; Ekechukwu, A.A.; Millike, C.E. Properties and function of pyomelanin. *Biopolymers* **2010**, *449*, 72.
4. Braconi, D.; Millucci, L.; Bernardini, G.; Santucci, A. Oxidative stress and mechanisms of ochronosis in alkaptonuria. *Free Radic. Biol. Med.* **2015**, *88*, 70–80. [CrossRef] [PubMed]
5. Chow, W.Y.; Norman, B.P.; Roberts, N.B.; Ranganath, L.R.; Teutloff, C.; Bittl, R.; Duer, M.J.; Gallagher, J.A.; Oschkinat, H. Pigmentation chemistry and radical-based collagen degradation in alkaptonuria and osteoarthritic cartilage. *Angew. Chemie Int. Ed.* **2020**, *59*, 11937–11942. [CrossRef]
6. Bernardus Mostert, A.; Davy, K.J.P.; Ruggles, J.L.; Powell, B.J.; Gentle, I.R.; Meredith, P. Gaseous adsorption in melanins: Hydrophilic biomacromolecules with high electrical conductivities. *Langmuir* **2010**, *26*, 412–416. [CrossRef]
7. Pradhan, S.; Brooks, A.K.; Yadavalli, V.K. Nature-derived materials for the fabrication of functional biodevices. *Mater. Today Bio* **2020**, *7*, 100065–100088. [CrossRef] [PubMed]
8. Caldas, M.; Santos, A.C.; Veiga, F.; Rebelo, R.; Reis, R.L.; Correlo, V.M. Melanin nanoparticles as a promising tool for biomedical applications–a review. *Acta Biomater.* **2020**, *105*, 26–43. [CrossRef] [PubMed]
9. D'Ischia, M.; Napolitano, A.; Pezzella, A.; Meredith, P.; Sarna, T. Chemical and structural diversity in eumelanins: Unexplored bio-optoelectronic materials. *Angew. Chemie Int. Ed.* **2009**, *48*, 3914–3921. [CrossRef]

10. Wang, Y.; Wang, X.; Li, T.; Ma, P.; Zhang, S.; Du, M.; Dong, W.; Xie, Y.; Chen, M. Effects of melanin on optical behavior of polymer: From natural pigment to materials applications. *ACS Appl. Mater. Interfaces* **2018**, *10*, 13100–13106. [CrossRef]
11. Manini, P.; Lino, V.; Franchi, P.; Gentile, G.; Sibillano, T.; Giannini, C.; Picardi, E.; Napolitano, A.; Valgimigli, L.; Chiappe, C.; et al. A robust fungal allomelanin mimic: An antioxidant and potent π-electron donor with free-radical properties that can be tuned by ionic liquids. *Chempluschem* **2019**, *84*, 1331–1337. [CrossRef]
12. Weidenfeld, I.; Zakian, C.; Duewell, P.; Chmyrov, A.; Ntziachristos, V.; Stiel, A.C. Homogentisic acid-derived pigment as a biocompatible label for optoacoustic imaging of macrophages. *Nat. Commun.* **2019**, *10*, 5056–5068. [CrossRef]
13. Janusz, G.; Pawlik, A.; Świderska-Burek, U.; Polak, J.; Sulej, J.; Jarosz-Wilkołazka, A.; Paszczyński, A. Laccase properties, physiological functions, and evolution. *Int. J. Mol. Sci.* **2020**, *21*, 966. [CrossRef]
14. Marcus, R.A.; Sutin, N. Electron transfers in chemistry and biology. *Biochim. Biophys. Acta* **1985**, *811*, 265–322. [CrossRef]
15. Eslami, M.; Namazian, M.; Zare, H.R. Electrooxidation of homogentisic acid in aqueous and mixed solvent solutions: Experimental and theoretical studies. *J. Phys. Chem. B* **2013**, *117*, 2757–2763. [CrossRef] [PubMed]
16. Joshi, R.; Gangabhagirathi, R.; Venu, S.; Adhikari, S.; Mukherjee, T. Antioxidant activity and free radical scavenging reactions of gentisic acid: In-vitro and pulse radiolysis studies. *Free Radic. Res.* **2012**, *46*, 11–20. [CrossRef] [PubMed]
17. Mostert, A.B.; Hanson, G.R.; Sarna, T.; Gentle, I.R.; Powell, B.J.; Meredith, P. Hydration-controlled X-band EPR spectroscopy: A tool for unravelling the complexities of the solid-state free radical in eumelanin. *J. Phys. Chem. B* **2013**, *117*, 4965–4972. [CrossRef]
18. Meredith, P.; Sarna, T. The physical and chemical properties of eumelanin. *Pigment Cell Res.* **2006**, *19*, 572–594. [CrossRef]
19. Panzella, L.; D'Errico, G.; Vitiello, G.; Perfetti, M.; Alfieri, M.L.; Napolitano, A.; D'Ischia, M. Disentangling structure-dependent antioxidant mechanisms in phenolic polymers by multiparametric EPR analysis. *Chem. Commun.* **2018**, *54*, 9426–9429. [CrossRef]
20. Sarna, T.; Plonka, P.M. Biophysical Studies of Melanin. In *Biomedical EPR, Part A: Free Radicals, Metals, Medicine, and Physiology*; Springer: Berlin, Germany, 2005; ISBN 978-0-387-26741-8.
21. Al Khatib, M.; Harir, M.; Costa, J.; Baratto, M.; Schiavo, I.; Trabalzini, L.; Pollini, S.; Rossolini, G.; Basosi, R.; Pogni, R. Spectroscopic characterization of natural melanin from a streptomyces cyaneofuscatus strain and comparison with melanin enzymatically synthesized by tyrosinase and laccase. *Molecules* **2018**, *23*, 1916. [CrossRef] [PubMed]
22. Schmaler-Ripcke, J.; Sugareva, V.; Gebhardt, P.; Winkler, R.; Kniemeyer, O.; Heinekamp, T.; Brakhage, A.A. Production of pyomelanin, a second type of melanin, via the tyrosine degradation pathway in Aspergillus fumigatus. *Appl. Environ. Microbiol.* **2009**, *75*, 493–503. [CrossRef] [PubMed]
23. Turick, C.E.; Tisa, L.S.; Caccavo, F. Melanin production and use as a soluble electron shuttle for Fe(III) oxide reduction and as a terminal electron acceptor by Shewanella algae BrY. *Appl. Environ. Microbiol.* **2002**, *68*, 2436–2444. [CrossRef]
24. Pralea, I.E.; Moldovan, R.C.; Petrache, A.M.; Ilieș, M.; Hegheș, S.C.; Ielciu, I.; Nicoară, R.; Moldovan, M.; Ene, M.; Radu, M.; et al. From extraction to advanced analytical methods: The challenges of melanin analysis. *Int. J. Mol. Sci.* **2019**, *20*, 3943. [CrossRef] [PubMed]
25. Taylor, A.M.; Vercruysse, K.P. Analysis of melanin-like pigment synthesized from homogentisic acid, with or without tyrosine, and its implications in alkaptonuria. *JIMD Rep.* **2017**, *35*, 79–85. [PubMed]
26. Tokuhara, Y.; Shukuya, K.; Tanaka, M.; Sogabe, K.; Ejima, Y.; Hosokawa, S.; Ohsaki, H.; Morinishi, T.; Hirakawa, E.; Yatomi, Y.; et al. Absorbance measurements of oxidation of homogentisic acid accelerated by the addition of alkaline solution with sodium hypochlorite pentahydrate. *Sci. Rep.* **2018**, *8*, 1–10. [CrossRef] [PubMed]
27. López, J.; Hernández-Alcántara, J.M.; Roquero, P.; Montiel, C.; Shirai, K.; Gimeno, M.; Bárzana, E. Trametes versicolor laccase oxidation of gallic acid toward a polyconjugated semiconducting material. *J. Mol. Catal. B Enzym.* **2013**, *97*, 100–105. [CrossRef]
28. Meng, X.; Crestini, C.; Ben, H.; Hao, N.; Pu, Y.; Ragauskas, A.J.; Argyropoulos, D.S. Determination of hydroxyl groups in biorefinery resources via quantitative 31P NMR spectroscopy. *Nat. Protoc.* **2019**, *14*, 2627–2647. [CrossRef]
29. Baiocco, P.; Barreca, A.M.; Fabbrini, M.; Galli, C.; Gentili, P. Promoting laccase activity towards non-phenolic substrates: A mechanistic investigation with some laccase-mediator systems. *Org. Biomol. Chem.* **2003**, *1*, 191–197. [CrossRef]
30. Pogni, R.; Baratto, M.C.; Teutloff, C.; Giansanti, S.; Ruiz-Dueñas, F.J.; Choinowski, T.; Piontek, K.; Martínez, A.T.; Lendzian, F.; Basosi, R. A tryptophan neutral radical in the oxidized state of versatile peroxidase from Pleurotus eryngii: A combined multifrequency EPR and density functional theory study. *J. Biol. Chem.* **2006**, *281*, 9517–9526. [CrossRef]
31. Pogni, R.; Teutloff, C.; Lendzian, F.; Basosi, R. Tryptophan radicals as reaction intermediates in versatile peroxidases: Multifrequency EPR, ENDOR and density functional theory studies. *Appl. Magn. Reson.* **2007**, *31*, 509–526. [CrossRef]
32. Brogioni, B.; Biglino, D.; Sinicropi, A.; Reijerse, E.J.; Giardina, P.; Sannia, G.; Lubitz, W.; Basosi, R.; Pogni, R. Characterization of radical intermediates in laccase-mediator systems. a multifrequency EPR, ENDOR and DFT/PCM investigation. *Phys. Chem. Chem. Phys.* **2008**, *10*, 7284–7292. [CrossRef]
33. Al Khatib, M.; Costa, J.; Baratto, M.C.; Basosi, R.; Pogni, R. Paramagnetism and relaxation dynamics in melanin biomaterials. *J. Phys. Chem. B* **2020**, *124*, 2110–2115. [CrossRef] [PubMed]
34. Panzella, L.; Gentile, G.; D'Errico, G.; Della Vecchia, N.F.; Errico, M.E.; Napolitano, A.; Carfagna, C.; D'Ischia, M. Atypical structural and π-electron features of a melanin polymer that lead to superior free-radical-scavenging properties. *Angew. Chemie Int. Ed.* **2013**, *52*, 12684–12687. [CrossRef] [PubMed]
35. Watt, A.A.R.; Bothma, J.P.; Meredith, P. The supramolecular structure of melanin. *Soft Matter* **2009**, *5*, 3754–3760. [CrossRef]
36. Pogni, R.; Baratto, M.C.; Sinicropi, A.; Basosi, R. Spectroscopic and computational characterization of laccases and their substrate radical intermediates. *Cell. Mol. Life Sci.* **2015**, *72*, 885–896. [CrossRef]

37. Carmieli, R.; Tadyszak, K. Electron spin relaxation studies of polydopamine radicals'. *J. Phys. Chem. B* **2021**, *125*, 841–849.
38. Grossmann, B.; Heinze, J.; Moll, T.; Palivan, C.; Ivan, S.; Gescheidt, G. Electron delocalization in one-electron oxidized aniline oligomers, paradigms for polyaniline. a study by paramagnetic resonance in fluid solution. *J. Phys. Chem. B* **2004**, *108*, 4669–4672. [CrossRef]
39. Chen, Z.; Bertin, R.; Froldi, G. EC50 estimation of antioxidant activity in DPPH* assay using several statistical programs. *Food Chem.* **2013**, *138*, 414–420. [CrossRef]

Supplementary material

Homogentisic acid and gentisic acid biosynthesized pyomelanin mimics: structural characterization and antioxidant activity

Maher Al-Khatib [1], Jessica Costa, [1] Daniele Spinelli, Eliana Capecchi[3], Raffaele Saladino[3], Maria Camilla Baratto[1] and Rebecca Pogni [1,*]

[1] Department of Biotechnology, Chemistry and Pharmacy, Via A. Moro 2, 53100 Siena; maher.al@unisi.it, jessica.costa2@unisi.it , mariacamilla.baratto@unisi.it, rebecca.pogni@unisi.it
[2] Next Technology Tecnotessile, Via del Gelso, Prato (Italy) 2; chemtech@tecnotex.it
[3] Department of Ecology and Biology, University of Tuscia, 01100 Viterbo, Italy; e.capecchi@unitus.it, saladino@unitus.it

* Correspondence: rebecca.pogni@unisi.it;

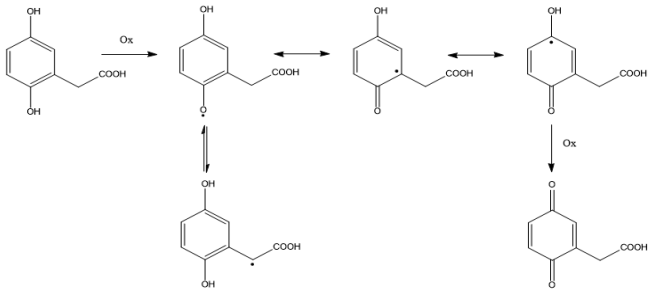

Scheme 1 – Scheme of the radical delocalization in HGA

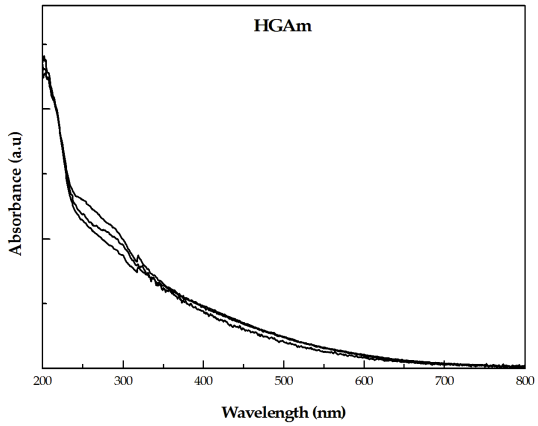

Fig S1: Reproducibility test of pyomelanin mimic from homogentisic acid (HGAm). The synthetic conditions were the same for all samples (pH 7.1 and molar ratio lac:HGA 1:1000). The UV-vis measurements were carried out at room temperature.

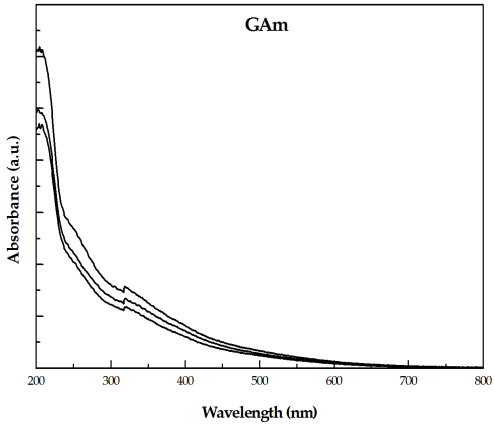

Fig S2: Reproducibility test of pyomelanin mimic from gentisic acid (GAm). The synthetic conditions were the same for all samples (pH 7.1 and molar ratio lac:GA 1:1000). The UV-vis measurements were carried out at room temperature.

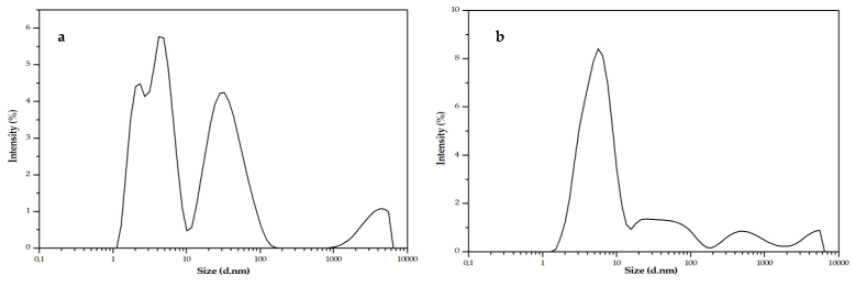

Fig. S3: DLS of a)HGAm and b) GAm. The spectra have been recorded in water.

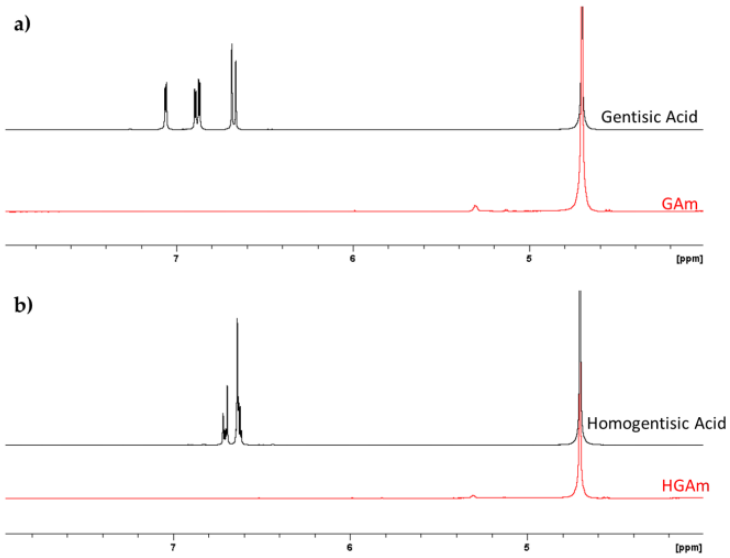

Fig. S4: In panel A: ^{1}H NMR spectra of GA (black line) and GAm (red line).
In panel B: ^{1}H NMR spectra of HGA (black line) and HGAm (red line).

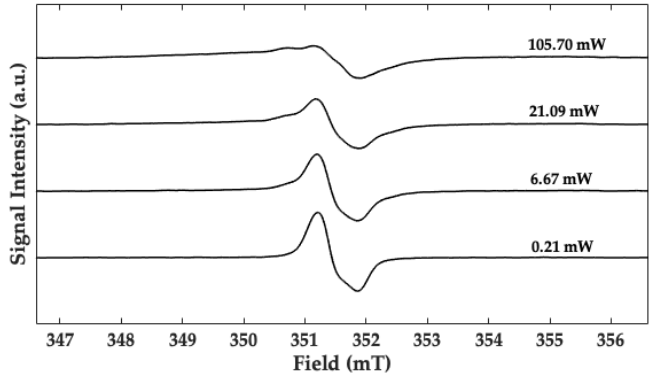

Fig. S5: Room temperature X-band (ν= 9.86 GHz) EPR spectra of GAm at pH 7.1 recorded at variable microwave power values.

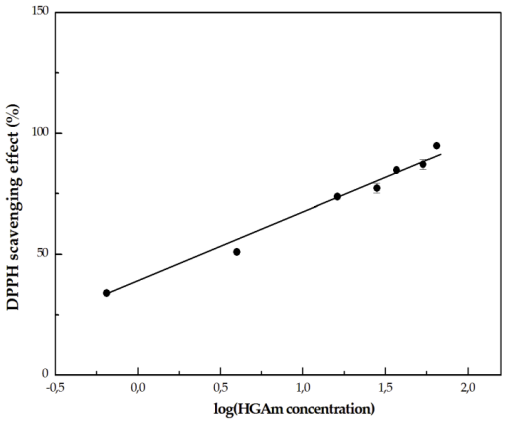

Fig. S6 Antioxidant activity of HGAm. The EC_{50} value was calculated using GraphPad Prism plotting the DPPH scavenger percentage measured by EPR spectroscopy in function of the log of HGAm concentrations analyzed. All measurements were repeated in triplicate.

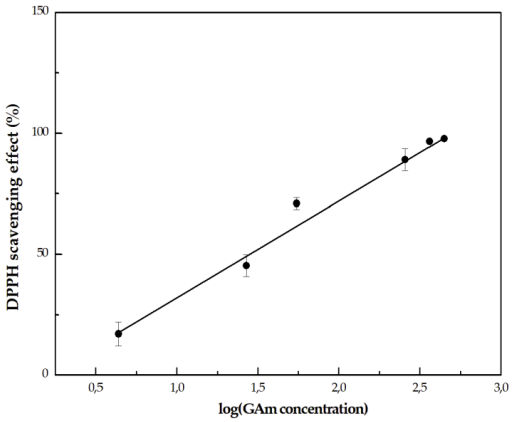

Fig. S7 Antioxidant activity of GAm. EC_{50} value was calculated using GraphPad Prism plotting the DPPH scavenger percentage measured by EPR spectroscopy in function of the log of GAm concentrations analyzed. All measurements were repeated in triplicate.

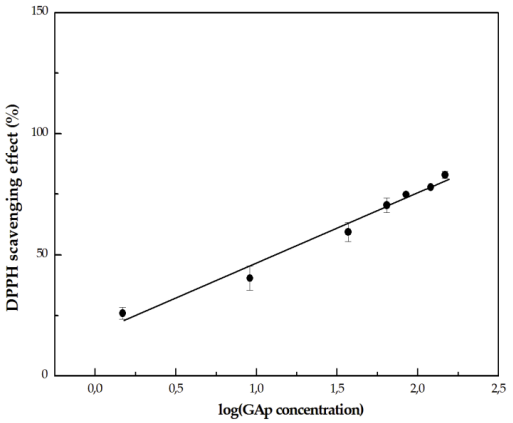

Fig. S8 Antioxidant activity of gallic acid polymer (GAp). The EC_{50} value was calculated using GraphPad Prism plotting the DPPH scavenger percentage measured by EPR spectroscopy in function of the log of GAp concentrations analyzed. All measurements were repeated in triplicate.

RSC Advances

ROYAL SOCIETY OF CHEMISTRY

PAPER

View Article Online
View Journal | View Issue

Check for updates

Cite this: *RSC Adv.*, 2021, **11**, 5529

Production and characterization of chitooligosaccharides by the fungal chitinase Chit42 immobilized on magnetic nanoparticles and chitosan beads: selectivity, specificity and improved operational utility†

Peter E. Kidibule,[a] Jessica Costa,[b] Andrea Atrei,[b] Francisco J. Plou,[c] Maria Fernandez-Lobato*[a] and Rebecca Pogni *[b]

Received 10th December 2020
Accepted 25th January 2021

DOI: 10.1039/d0ra10409d

rsc.li/rsc-advances

Chitin-active enzymes are of great biotechnological interest due to the wide industrial application of chitinolytic materials. Non-stability and high cost are among limitations that hinder industrial application of soluble enzymes. Here we report the production and characterization of chitooligosaccharides (COS) using the fungal *exo*-chitinase Chit42 immobilized on magnetic nanoparticles and food-grade chitosan beads with an immobilization yield of about 60% using glutaraldehyde and genipin linkers. The immobilized enzyme gained operational stability with increasing temperature and acidic pH values, especially when using chitosan beads-genipin that retained more than 80% activity at pH 3. Biocatalysts generated COS from colloidal chitin and different chitosan types. The immobilized enzyme showed higher hydrolytic activity than free enzyme on chitosan, and produced COS mixtures with higher variability of size and acetylation degree. In addition, biocatalysts were reusable, easy to handle and to separate from the reaction mixture.

Introduction

Chitin is a renewable and biodegradable semi crystalline biopolymer mainly formed by *N*-acetyl-β-D-glucosamine (GlcNAc) units. It is the most abundant polysaccharide of the marine environment and the second (after cellulose) on the earth. This ubiquitous material offers strength to the exoskeleton of insects and arthropods and it is an essential component of fungi cell walls. The deacetylated form of chitin is chitosan, polysaccharide composed of fully or partial deacetylated β-(1-4)-linked GlcNAc units. Both chitin and chitosan are large biopolymers, with molecular size depending on the producing organism and the method of their production.[1] Sustainability, renewability, availability and other benefits of chitinolytic polymers seemed to be the solution for the critical problem faced worldwide on waste disposal and management by reducing hundreds of millions of tons of synthetic polymers produced annually.[1,2] The hydrolysis of chitin and chitosan to produce chitooligosaccharides (COS) (MW 2–30 kDa) can be carried out chemically, physically, or enzymatically, the first being the most used strategy and the latter the most specific, controllable and environmentally friendly option.[3] COS are soluble in aqueous solutions and show biocompatibility and biodegradability properties. Furthermore, they show more prominent antiviral, antibacterial, antitumor and antioxidant activities than chitin and high molecular weight chitosan making them gain value in the biotechnological sector. The biological activity of COS depending on their size, degree and pattern of acetylation.[4–6] Specific enzymes such as chitinases and chitosanases, or unspecific such as carbohydrases and proteases have been employed in conversion of chitin and chitosan to COS.[7,8] Chitinases (E.C 3.2.2.14) are extensively distributed Glycoside Hydrolases (GH), which cleave at internal or terminal β-(1-4) glycosidic linkages of chitin. These enzymes are structurally included in GH families 18, 19 and 20 (http://

[a]*Department of Molecular Biology, Centre for Molecular Biology Severo Ochoa (CSIC-UAM), University Autonomous from Madrid, Nicolás Cabrera, 1. Cantoblanco, 28049 Madrid, Spain. E-mail: mfernandez@cbm.csic.es*

[b]*Department of Biotechnology, Chemistry and Pharmacy, Università di Siena, Via A. Moro 2, 53100 Siena, Italy*

[c]*Institute of Catalysis and Petrochemistry, CSIC, Marie Curie, 2. Cantoblanco, 28049 Madrid, Spain*

† Electronic supplementary information (ESI) available: Fig. S1. MALDI-TOF MS analysis of COS produced from chitosan CHIT600. Table S1. Main peaks and intensities of the mass spectrum corresponding to the reaction mixture obtained with colloidal chitin as substrate and MNPs-Ga-Chit42. Table S2. Main peaks and intensities of the mass spectrum corresponding to the reaction mixture obtained with colloidal chitin as substrate and CMS-Ga-Chit42. Table S3. Main peaks and intensities of the mass spectrum corresponding to the reaction mixture obtained with chitosan QS2 as substrate and MNPs-Ga-Chit42. Table S4. Main peaks and intensities of the mass spectrum corresponding to the reaction mixture obtained with chitosan QS2 as substrate and CMS-Ga-Chit42. See DOI: 10.1039/d0ra10409d

www.cazy.org) that are present in all organism kingdoms.[8,9] *Exo*-chitinases attack the polysaccharide from the non-reducing end of the polymer chain releasing the disaccharide chitobiose (di-acetyl-glucosamine $(GlcNAc)_2$) as major product, whereas *endo*-enzymes attack randomly from internal points along the polysaccharide producing tetrasaccharides and higher size sugars as majority products.[9,10] As mentioned above, enzymatic methods for production of COS are the most interesting alternative for the industrial sector, but undoubtedly, yields of the products obtained in hydrolytic reactions are still far from being suitable. In fact, only less than 25% of the substrate is usually transformed into products by free chitinases, which makes industries to use less environmentally friendly strategies to produce COS.[6] Immobilization of enzymes constitutes a powerful tool to improve some biocatalyst limitations such as their stability, high cost production cycle and low productivity levels.[11–13] Over other types of support systems used in immobilization, the use of Magnetic Nanoparticles (MNPs) of 10 to 20 nm shows advantages like non-toxicity, large surface area and surface volume ratio or the simplicity in separating the biocatalyst after use. In addition, the MNPs surface can be modified coating with different compounds such as (3-amino-propyl) triethoxysilane (APTES). In this way, the amino group on their surface allows the attack of linker such as glutaraldehyde (GA), to facilitate the protein binding. Attachment of enzymes on chitosan beads is also a widely used immobilization method and different chitosan-based supports have been reported given the biodegradable and environmentally friendly nature of this material. The presence of active amino groups in deacetylated GlcNAc units of chitosan also enables the binding of GA and that of proteins. In addition, Chitosan beads/Macro-Spheres (CMS) employ centrifugation or filtration for separation of the catalysts from the reaction mixture. Therefore, some chitosanases, lipases, amylases and laccases (among others) have been already immobilized using MNPs and/or CMS with successful results.[11,14–18] In contrast, most chitinases previously immobilized using both types of supports lost their activity after being reused in consecutive cycles or no data concerning production and characterization of COS were reported.[19–21] Chitinase Chit42 from the fungus *Trichoderma harzianum* was previously expressed in the yeast *Pichia pastoris* with about 3 g L^{-1} of the protein produced in this heterologous system. This fungal *exo*-chitinase of the family GH18 hydrolyzed chitin oligomers with a minimal degree of polymerization (DP) of 3 units, with chitobiose being the main hydrolysis product.[8] Chitosan and COS are produced and commercialized by different companies as safe dietary supplements.[22] They are Generally Recognized As Safe (GRAS) compounds also at high dietary concentrations in animals and humans. However, the extraordinary biological activity of COS requires to identify new methods for production, purification and characterization. The goal of this work is to produce and characterize COS with the immobilized biocatalyst for the bioconversion of colloidal chitin and chitosan polymers. In addition, the reusability of the immobilized biocatalyst has also been evaluated.

Results and discussion

Morphology and size of MNPs, before and after immobilization of Chit42, were analyzed using TEM. The MNPs were rough spheres with an average diameter of about 10 nm that formed scattered groups due to the forces of attraction between them, and which remain even after sonication (Fig. 1A). The nanoparticles with the supported enzyme, MNPs-GA-Chit42, are visualized in Fig. 1B. All complexes apparently showed the same size and shape to each other and to that previously obtained in other works[23,24] even if particles larger than 20 nm have also been reported before.[16]

Chitosan beads produced in this study were clear macrospheres that proved to be stable in conditions used in enzymatic assays. The size of wet and dry chitosan beads was of about 2 mm and apparently 1 mm, respectively, by using millimeter paper (data not shown). Dry spheres were also analyzed using SEM and showed a size of 0.99 mm. Initially, 0.5% GA or 0.125% Gpn and different ratios of protein (Chit42) per gram of support were used. Best results of immobilization on MNPs were obtained using 6.2 mg of protein, where the immobilization yield and the recovered hydrolytic chitinase activity were both of around 62–67% (Table 1), and with less than 50% of recovery activity when using higher or lower amounts of proteins (see information in the Table 1 footnote). When chitinase Chit42 was immobilized on chitosan beads using GA or Gpn, best results were obtained using 6.2 and 2 mg of protein/g of CMS beads, with a recovery activity of 71% and 62%, respectively (Table 1), and less than 40% and 60% of recovery activity for CMS-GA and CMS-Gpn, respectively, when other conditions were used (Table 1). The selection of MNPs and CMS beads as supporting materials were motivated by the fact that in the first case the products can be easily separated from the medium while CMS beads are more sustainable to be used for food purposes. Furthermore with CMS, different linkers, GA and

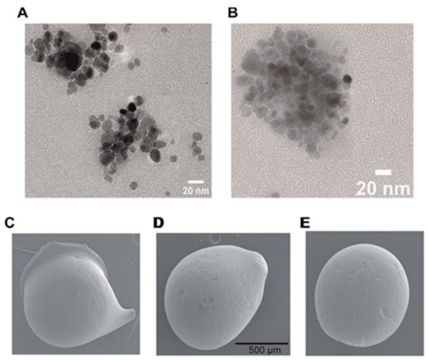

Fig. 1 TEM and SEM analyses of generated supports. TEM images of magnetic nanoparticles. (A) MNPs-GA and (B) MNPs-GA-Chit42. SEM images of dry chitosan macrospheres of (C) CMS-GA, (D) CMS-GA-Chit42 and (E) CMS-Gpn-Chit42. GA 0.5% and Gpn 0.125% were used. Scale bars are showed; same scale in (C) and (E) as in (D).

Gpn, have been tested for their different structure and chain length and because the latter is a natural and completely atoxic linker. To our knowledge, partial information is available on immobilized chitinases from different sources using MNPs and CMS beads in literature but no information on the production and detailed characterization of the produced COS by immobilized enzymes are reported. Thus, a recombinant chitinase was already immobilized using carboxyl functional MNPs with immobilization yield of 64%, which showed activity against the fungi *Botrytis cinerea*[25] and a commercial chitinase from *Trichoderma viride* on superparamagnetic particles using a rotational magnetic field with no activity/immobilization yields reported.[26] Chitosan beads and GA have also been used to immobilize chitinases such as that from *Streptomyces griseus* and *Paenibacillus illinoisensis*, with an immobilization yield of about 42%,[19] and a thermostable enzyme from *Thermomyces lanuginosus* with almost 100% of immobilization yield but without data of the activity recovery reported.[20] In addition, different polymers have also been previously used to immobilize chitinolytic enzymes. Among them, hydroxypropyl methylcellulose acetate succinate for a commercial chitinase from *Serratia marcescens*, with an immobilization yield of 78% and recovery activity of 41%[27] and k-carrageenan-alginate gel for chitinase from *Aspergillus awamori* with immobilization and recovery activity yields of 93% and 77%, respectively.[28] A lower immobilization yield (25%) was also obtained by covalent immobilization of a chitinolytic activity of *Bacillus amyloliquefaciens* in glyoxal agarose beads.[29] Similar to free Chit42, the immobilized enzyme on MNPs displayed maximum activity at 35–40 °C but *a priori* could be more thermostable because retained more than 60% of its activity after 1 h at 50 °C (Fig. 2B) instead of about 20% retained by the non-immobilized enzyme (Fig. 2A). Immobilization on chitosan beads also increases the thermal activity profile of Chit42, which showed an optimal temperature of 45 °C and retained 50% of its activity at 50 °C (Fig. 2B). This stabilization effect is well-reported in covalent immobilization.[30] Concerning the pH dependence, free enzyme showed optimal activity at pH 5.0–6.0 (Fig. 2A). However, the activity of the immobilized Chit42 increased remarkably at acidic pH values, and specially, when using chitosan beads and Gpn, which showed maxima activity at pH 4 and retained more than 80% of the activity at pH 3 (Fig. 2C). The formation of

Table 1 Optimal immobilisation condition for chitinase Chit42[a]

Support type	Chit42 (mg g^{-1} support)	Immobilization yield (%)	Recovery of activity (%)
MNPS-GA	6.2	62.3	66.7
CMS-GA	6.2	57.0	71.0
CMS-GPN	2.0	86.5	62.3

[a] 100% activity: 32.2, 32.2 and 10.4 U g^{-1} of biocatalyst for MNPs-GA, CMS-GA and CMS-Gpn, respectively. GA 0.5% and Gpn 0.125%. For: 3.12, 6.2, 12.4, 24.8 mg g^{-1} MNPs-GA, immobilization yields: 56.1, 62.3, 43.2, 23% and recovery activity: 46.5, 66.7, 38.3, 19%. For 0.78, 1.55, 3.1, 6.2 mg g^{-1} CMS-GA, immobilization yields: 17.4, 32.4, 53.7, 57% and recovery activity: 4.7, 13.2, 34.6, 71%. For 0.5, 1.5, 2, 2.5 mg g^{-1} CMS-Gpn, immobilization yields: 28, 70.7, 86.6, 64.5% and recovery activity: 43.4, 50.1, 62.3, 55.7%; all respectively.

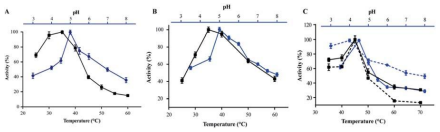

Fig. 2 Temperature and pH dependence profiles of the free and immobilized chitinase activity. (A and B) Temperature (black) and pH (blue) profiles for the free and the linked to MNPs-GA enzyme, respectively. (C) Temperature (black) and pH (blue) when CMS-GA (continuous line) and CMS-Gpn (discontinuous line) supports were used. Data are means of three independent values. Standard errors are indicated.

covalent bond through amino groups of the immobilized Chit42 can cause imbalanced partition of H^+ and OH^- concentrations resulting in the protein higher acidic stability.[31] In any case, the higher apparent acidic stability of the immobilized Chit42 gives this biocatalyst the advantage to act more efficiently on chitin and chitosan, which are more soluble at low pH values. The reuse of enzymes in industrial processes is of enormous economic relevance. The reusability of chitinase Chit42 immobilized on MNPS and CMS was investigated using batch reactions (Fig. 3). After each cycle of reaction (1 h), catalysts MNPs-GA-Chit42 and CMS-GA/Gpn-Chit42 were separated from their reaction mixtures using external magnetic field and centrifugation, respectively. Before every one of the new reused cycles, all catalysts were washed in distilled water and phosphate buffer. The catalyst MNPs-GA-Chit42 retained higher than 70% of its initial chitinolytic activity after 2 cycles but only 30% after 5 cycles (Fig. 3A). However the catalyst CMS-GA-Chit42 completely lost its activity after the second cycle, which made us to test also Gpn as linker, but CMS-Gpn-Chit42 retained only about 30% of the initial activity (Fig. 3B), a value still clearly lower than that obtained with MNPs. In addition, the loss of activity during recovery steps due to possible outflow of the enzyme from the support was also investigated, but no free enzyme was detected on the washing buffer. Loss of chitinase activity after immobilization on MNPs and CMS has been previously reported using commercial chitinases, which retained less of 20% of their initial activity after only 2 reuse cycles.[19,26] Nevertheless to stabilize bonds between enzymes and supports, the reduction with sodium borohydride, which

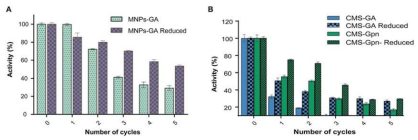

Fig. 3 Reusability of immobilized Chit42 on (A) MNPs and (B) CMS supports. Relative activity was evaluated on colloidal chitin. The 100% activity was 33.3, 28.9, 66.7, 23.3, 72.2 and 48.3 units per g of biocatalyst for MNPs-GA, MNPs-GA-reduced, CMS-GA, CMS-GA-reduced, CMS-Gpn and CMS-Gpn-Reduced, respectively. GA/Gpn-reduced with $NaBH_4$. Assays were conducted in triplicate and data are means of three parallel measurements. Standard errors are indicated.